Chemical Engineering Science, Vol. 43, No. 3, pp. 451–457, 1988.
Printed in Great Britain.

0009–2509/88 $3.00 + 0.00

LIQUID CIRCULATION IN AIRLIFT REACTORS

M. Y. CHISTI, B. HALARD and M. MOO-YOUNG
Department of Chemical Engineering, University of Waterloo, Waterloo, Ontario N2L 3G1, Canada

(*Received* 11 *March* 1987; *accepted for publication* 22 *June* 1987)

Abstract—Energy balance over an airlift loop is used to obtain a theoretical equation [eq. (16)] for the prediction of liquid circulation velocity in those devices. The resulting equation is shown to satisfactorily describe most of the available liquid circulation data (13 different airlift reactors) for a large range of reactor operating scales (0.06–1.06 m^3 liquid volumes) including measurements on two pilot scale vessels. The equation applies to both external- and internal-loop types of airlifts over almost two decades of liquid circulation velocities (0.027–1.05 $m\,s^{-1}$), reactor height range of 1.36–8.5 m, and riser-to-downcomer cross-sectional area ratios in the range 0.5–9.1. The liquid circulation rate is predicted to increase with the square root of the reactor height. The influence of wall-drag on liquid circulation is shown to be negligible relative to the impact of the frictional losses in the top and bottom connecting sections between the riser and the downcomer where abrupt changes of flow direction take place. Energy dissipation due to wakes behind rising bubbles is most significant.

INTRODUCTION

Airlift reactors are gas–liquid (or slurry) contacting devices which are of particular importance in biotechnology industries. In general, these reactors are made up of a pool of liquid divided into two vertical zones connected at the top and bottom. One of these zones (the riser) is sparged by a gas and the resulting gas holdup difference between the gas-sparged riser and the unsparged downcomer leads to a difference in the bulk densities of the fluids in the two zones and hence an induced fluid circulation—upflow in the riser, downflow in the downcomer—is set up. The magnitude of liquid circulation is one of the most important design and scale-up parameters for airlift reactors: liquid circulation influences the gas holdup in the vessel, the prevailing flow regime, heat and mass transfer coefficients, and the extent of mixing in the reactor.

This paper reports on a model for prediction of liquid circulation velocity in airlift devices and on the influence of reactor geometry on liquid circulation. Experimental data obtained by various authors over a very broad range of airlift reactor sizes and reactor types, including our data on two pilot scale devices, are shown to agree with the model.

LITERATURE

A combination of momentum balance over the circulation loop with empirical gas holdup and two-phase pressure drop correlations is one approach to predicting liquid circulation velocity in airlift reactors. At steady state the hydrostatic pressure difference driving force for the circulation resulting from the gas holdup difference between the riser and the downcomer is balanced by the total pressure drop in the circulation path due to friction, valves, bends, flow area changes and the presence of internals. This procedure for liquid velocity prediction and its modifications were employed by Hsu and Dudukovic (1980), Chakravarty *et al.* (1974), Kubota *et al.* (1978), Blenke (1979), Merchuk and Stein (1981), Bello (1981) and Jones (1985). In all cases either the predicted liquid velocity did not satisfactorily compare with the observed value or the equation involved a large amount of empiricism such as the two-phase flow friction factors. The relatively simple theoretical equation reported by Jones (1985) (eq. 18 of his paper) also predicted significantly higher or lower values of liquid circulation velocity than the experimentally found ones. Also, the energy losses due to drag of gas bubbles in the downcomer were neglected. In another study Bello *et al.* (1984) theoretically related (via an energy balance on the airlift loop) the riser linear liquid velocity V_{Lr} to the riser superficial gas velocity by

$$V_{Lr} = (2gh_D U_{Gr}/\eta)^{1/3} \tag{1}$$

where η is the total circulation path flow resistance in the flow circuit. For correlating their experimental data, however, Bello *et al.* (1984) used equations of the form

$$V_{Lr} = \alpha(A_d/A_r)^{\beta} U_{Gr}^{1/3}. \tag{2}$$

The values of β were about 0.75 and were largely independent of the reactor or contactor type (whether external loop airlift or internal concentric draught tube device). However, α depended on the type of contactor and α values of 1.55 (external loops) and 0.66 (concentric draught tube internal loops) were reported. This meant that more than two-fold higher liquid circulation rates were obtained in the external-loop devices (where there was a relatively low downcomer gas holdup) compared with the internal loop draught tube vessels in which the gas entrainment in the downcomer was higher. This confirms that downcomer gas holdup must also be taken into account in liquid velocity predictions. Equations (1) and (2) taken together imply that the downcomer-to-riser cross-sectional area ratio was the principal factor which controlled η, the total circulation path flow resistance, and that wall friction was less important since fluid viscosity did not appear in eq. (1). In almost the same geometries and sizes of external-loop vessels as used by Bello et al. (1984) other investigations (Popovic and Robinson, 1984) conducted in non-Newtonian carboxymethyl cellulose solutions (μ_{app} of 0.015–0.5 Pa s) showed that

$$U_{Lr} = \alpha U_{Gr}^{0.322} (A_d/A_r)^{0.794} \mu_{app}^{0.395} \tag{3}$$

where α was 0.052 and 0.0204 for bubble- and slug-flow regimes, respectively. The exponents on gas velocity and geometric terms in eqs (2) and (3) are quite close, thereby indicating that these exponents are largely independent of fluid properties. The decline in liquid circulation with increasing viscosity observed by Popovic and Robinson (1984), Weiland (1984), Onken and Weiland (1980) and Chakravarty et al. (1974) both in Newtonian and non-Newtonian media probably meant that wall friction losses became important as viscosity increased relative to that in water-like fluids. The report of Fields et al. (1984) that addition of small amounts of drag-reducing polymers such as xanthan gums enhanced liquid circulation compared to the value in water may be similarly explicable. The effects of viscosity- and drag-reducing agents on liquid circulation have another explanation in terms of energy dissipation in the circulating fluid in the bubble wakes.

Recently Lee et al. (1986) presented an analysis of the liquid circulation phenomenon in airlift contactors. The energy losses in the wakes behind bubbles in the riser as well as the losses in the downcomer due to upflow of large bubbles were taken into account. The predicted circulation velocities were found to agree satisfactorily with the experimentally observed values, but the calculation required a knowledge of terminal bubble rise velocity. Lee et al. (1986) used an arbitrary, but realistic, value of 0.23 m s^{-1} for the terminal bubble rise velocity in most of their calculation. In some cases, however, to achieve satisfactory agreement between the model and experimental results they had to adjust the bubble rise velocity and consequently the bubble velocities used varied almost two-fold over the range 0.22–0.43 m s^{-1}, with little justification. Thus the bubble rise velocity was used as merely an adjustible parameter without any real physical meaning. In addition, these investigators assumed quite arbitrary values of frictional loss factors, between 2 and 4, for the various airlift devices despite the wide variations in reactor geometries.

In view of the shortcomings of existing liquid circulation studies for airlift vessels, and considering their lack of generality, we have developed a new liquid circulation model which is presented here. The model is shown to be universally applicable to all types of airlift reactors: external loop, split cylinder internal loop, and annulus or draught tube sparged concentric draught tube internal loop geometries.

THEORY

The energy balance over an airlift loop may be written as

rate of energy input into reactor = rate of energy dissipation or

$$E_i = E_R + E_D + E_B + E_T + E_F \tag{4}$$

where

E_i = energy input due to isothermal gas expansion

$$= QP_h \ln\left(1 + \frac{\rho_D g h_D}{P_h}\right) \tag{5}$$

E_R = energy dissipation due to wakes behind bubbles in the riser

E_D = energy loss due to stagnant gas in the downcomer

$E_{B(T)}$ = energy loss due to fluid turn around at the bottom (top) of reactor

E_F = energy loss due to friction in the riser and the downcomer.

For simplicity only Newtonian low-viscosity (water-like) flows will be considered. Under these conditions it may be shown (Appendix 1) that skin or wall friction losses in airlift vessels are negligible compared to dissipation due to other terms in eq. (4). This is true in general for low-viscosity fluids as confirmed further by the data presented by Lee et al. (1986). Thus we shall ignore skin friction losses.

Energy dissipation due to the wakes behind the bubbles in the riser can be obtained by an energy balance using the riser liquid as the control volume. Thus

$$E_i = E_R - \underbrace{\rho_L g h_D (1-\varepsilon_r) U_{Lr} A_r}_{\text{pressure energy loss}} + \underbrace{\rho_L g h_D U_{Lr} A_r}_{\text{potential energy gain}}. \tag{6}$$

Hence

$$E_R = E_i - \rho_L g h_D U_{Lr} A_r \varepsilon_r. \tag{7}$$

Energy loss arising from the drag of gas on liquid in the downcomer (E_D) is obtained by performing an energy balance on the downcomer, using the downcomer liquid as the control volume:

$$0 = E_D + \underbrace{\rho_L g h_D (1-\varepsilon_d) U_{Ld} A_d}_{\text{pressure energy gain}} - \underbrace{\rho_L g h_D U_{Ld} A_d}_{\text{potential energy loss}} \tag{8}$$

or

$$E_D = \rho_L g h_D U_{Ld} A_d \varepsilon_d. \tag{9}$$

The energy losses in the top and bottom sections of the airlift reactor can be calculated in exactly the same way as for pipe flow. Thus

$$E_B + E_T = \tfrac{1}{2}\rho_L[V_{Lr}^3 K_T A_r (1-\varepsilon_r) + V_{Ld}^3 K_B A_d (1-\varepsilon_d)] \tag{10}$$

where K_T and K_B are the friction loss coefficients for the top and bottom connecting sections, respectively. V_{Lr} and V_{Ld} in eq. (10) are the true linear liquid velocities in the riser and the downcomer, respectively, and are related to the corresponding superficial velocities in the following manner:

$$V_{Lr} = \frac{U_{Lr}}{1-\varepsilon_r} \tag{11}$$

$$V_{Ld} = \frac{U_{Ld}}{1-\varepsilon_d}. \tag{12}$$

Furthermore, the continuity equation for the liquid flow between the riser and the downcomer can be written as

$$A_r(1-\varepsilon_r)V_{Lr} = A_d(1-\varepsilon_d)V_{Ld}. \tag{13}$$

Using eqs (11) and (13) in (10) we obtain

$$E_B + E_T = \tfrac{1}{2}\rho_L U_{Lr}^3 A_r\left[\frac{K_T}{(1-\varepsilon_r)^2} + K_B\left(\frac{A_r}{A_d}\right)^2 \frac{1}{(1-\varepsilon_d)^2}\right]. \tag{14}$$

Finally, substitution of eqs (7), (9) and (14) in eq. (4) yields the following expression

$$E_i = E_i - \rho_L g h_D U_{Lr} A_r \varepsilon_r + \rho_L g h_D U_{Lr} A_r \varepsilon_d + \tfrac{1}{2}\rho_L U^3_{Lr} A_r\left[\frac{K_T}{(1-\varepsilon_r)^2} + K_B \times \left(\frac{A_r}{A_d}\right)^2 \frac{1}{(1-\varepsilon_d)^2}\right]. \tag{15}$$

Equation (15) can be written in terms of U_{Lr} explicitly:

$$U_{Lr} = \left[\frac{2gh_D(\varepsilon_r - \varepsilon_d)}{\dfrac{K_T}{(1-\varepsilon_r)^2} + K_B\left(\dfrac{A_r}{A_d}\right)^2 \dfrac{1}{(1-\varepsilon_d)^2}}\right]^{0.5}. \tag{16}$$

Equation (16) is our general equation for liquid velocity prediction in airlift reactors. Two further simplified particular forms of eq. (16) may be distinguished. For split cylinder or concentric tube type internal loop airlift devices the energy loss in the top connecting section will usually be minimal relative to that in the bottom section. This is because the internal loop reactor headspace may be likened to an open channel as opposed to a constricted flow path at the bottom. In this case we have

$$U_{Lr} = \left[\frac{2gh_D(\varepsilon_r - \varepsilon_d)}{K_B\left(\dfrac{A_r}{A_d}\right)^2 \dfrac{1}{(1-\varepsilon_d)^2}}\right]^{0.5}. \tag{16a}$$

On the other hand, for an external-loop type of airlift where, as is often the case, the top and bottom connections are very similar in geometry, K_T and K_B are approximately equal. In this case eq. (16) reduces to

$$U_{Lr} = \left[\frac{2gh_D(\varepsilon_r - \varepsilon_d)}{K_B\left(\dfrac{1}{(1-\varepsilon_r)^2} + \left(\dfrac{A_r}{A_d}\right)^2 \dfrac{1}{(1-\varepsilon_d)^2}\right)}\right]^{0.5}. \tag{16b}$$

Equations (16), (16a) and (16b) incorporate the diameter of the riser in terms of the superficial liquid velocity in the riser. The riser (or downcomer) diameter is a necessary geometric detail for the prediction of liquid velocity in airlift reactors because the A_r/A_d ratio by itself does not uniquely define the reactor geometry. The additional requirement of dimensional consistency is satisfied by eqs (16)–(16b).

EXPERIMENTAL

Liquid circulation time was measured in an air–water system in a 1.46-m^3 pilot scale airlift device which consisted of a cylindrical, 0.762 m diameter, 3.21 m tall, all-steel vessel containing a concentric draught tube, 0.355 m in internal diameter. The draught tube (downcomer) was 2.06 m tall and it was located 0.202 m from the base of the reactor. The unaerated liquid height was kept at 2.32 m and the annular space (riser) between the outer and inner tubes was sparged by a perforated pipe (128 holes of 0.002 m diameter on three concentric rings) type sparger.

Concentrated sulphuric acid was used as a tracer which was poured instantaneously into the top of the downcomer and the pH was followed at two downstream locations by identical pH probes placed about 2 m apart in the downcomer. From the measured time interval between the tracer peaks from the two pH electrodes and the known vertical distance between them the linear liquid velocity in the downcomer could be calculated. A similar method was used also by Verlaan *et al.* (1986).

A second reactor—a split cylinder—was also investigated using air–water. This consisted of a circular clear plastic column, 0.243 m in diameter, 7.825 m tall, split vertically into a riser and downcomer by a 4.8 m tall, 0.229 m wide, aluminium baffle. The baffle clearance from the bottom of the reactor was 0.102 m and a clear liquid height of 5.076 m was used giving a liquid volume of 0.2354 m^3 and a top baffle clearance of 0.174 m. The A_r/A_d ratio was 2.44. The riser was sparged by a perforated pipe sparger (38 holes, 0.0015 m diameter). In this case the downcomer liquid velocity was calculated from the simpler visual observations of the bubble size for bubbles held stationary in the lower part of the downcomer due to downflow of liquid. The well-known Levich (1962) equation

$$U_{Ld} = 2\left(\frac{gd_B}{1.8}\right)^{0.5} \tag{17}$$

was then used to calculate the flow past the bubble. Glasgow *et al.* (1984) have successfully utilized this technique.

RESULTS AND DISCUSSION

The liquid circulation data for our airlift reactors is shown in Fig. 1 together with almost all other data available on liquid circulation in airlift devices, both external- and internal-loop types. Experimental values of superficial liquid velocity in the riser are plotted against those calculated using either eq. (16a) (for internal loops) or eq. (16b) (for external loops). Figure 1 shows that over almost two decades of liquid velocity range in airlift contactors and over a large reactor size

Table 1. Geometric details of airlift reactors

No.	Description	V_L (m^3)	h_L, h_D or reactor height (m)	d_r or equivalent hydraulic diameter (m)	d_d or equivalent hydraulic diameter (m)	A_r/A_d (–)	L_r (m)	L_d (m)	L_b (m)	K_B (–)	Reference
1	DT internal loop (annulus sparged)	1.058	2.32	0.407	0.355	3.61	—	2.06	0.202	5.0	This work
2	Split cylinder (internal loop)	0.2354	5.076	0.19	0.102	2.44	5.076	5.076	0.102	7.38	This work
3	DT internal loop (DT sparged)	0.20	2.80	0.206	0.094	0.892	2.60	—	0.033	16.98 ± 3.74	Hatch (1973)
4	DT internal loop (DT sparged)	0.06	1.33	0.146	0.104	0.541	1.22	—	0.100	9.22 ± 0.47	Jones (1985)
5a	DT internal loops	~ 0.033	1.80	0.101	0.051	7.692			0.10	4.92 ± 2.77	Bello (1981)
b	(annulus sparged)	(dispersion		0.076	0.076	2.857	1.80	1.55			
c	(three reactors)	volume)		0.063	0.089	1.786					
6	External loop	0.3 (total volume)	~ 4.05	0.14	0.14	1.00	4.05	4.05	—	5.43 ± 0.13	Merchuk and Stein (1981)
7	External loop	0.165	3.23	0.20	0.10	4.0	3.23	3.23	—	1.81 ± 0.08	Verlaan *et al.* (1986)
8	External loop	~ 0.08 (dispersion volume)	8.5 (reactor height = 10 m)	0.100	0.050	4.0	~ 8.5	~ 8.5	—	4.98 ± 0.21	Onken and Weiland (1980)
9a	External loops	~ 0.041	1.80	0.152	0.051	9.091	1.55	1.55	—	6.09 ± 0.96	Bello (1981)
b	(three reactors)	to 0.056			0.076	4.000					
c		(dispersion volume)			0.102	2.273					

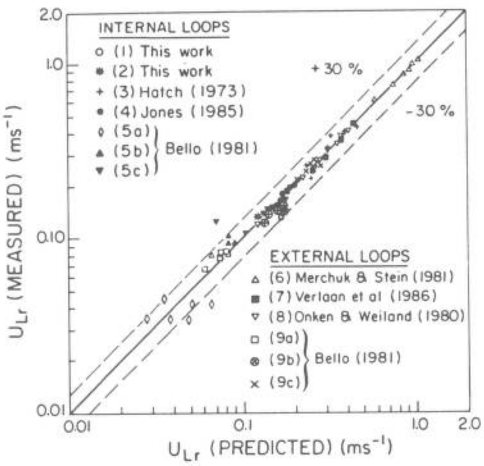

Fig. 1. Measured superficial liquid velocity in riser vs predicted value [eq. (16a) or (16b)]. For details of reactors see Table 1.

range (0.06–1.06 m^3 liquid volume) eq. (16) predicts liquid velocity very well ($\pm 30\%$).

The values of the form frictional loss coefficient K_B used in eqs (16a) and (16b) are tabulated in Table 1 along with other geometric details for various reactors referred to in Fig. 1. As expected, for any given reactor K_B is constant within narrow limits. Variation of K_B between *different* reactors is expected because of the different reactor geometries. Notice also that for some seemingly very different external-loop reactors—all those used by Bello (1981), the one used by Merchuk and Stein (1981), and the very tall vessel employed by Onken and Weiland (1980)—K_B is almost the same at ~ 5.5. This is because the bottom sections of all these vessels were similar in geometry. For example, the risers and downcomers of Bello's vessels were connected by a ~ 10.2 cm diameter pipe while Merchuk and Stein (1981) apparently used a connecting pipe of 14 cm diameter. Also the lengths of the connecting pipes in the two cases were quite close at ~ 0.5 m for Bello (1981) and 0.35 m for the vessel used by Merchuk and Stein (1981). Because Bello's device was only about 1.8 m tall whereas that used by Merchuk and Stein (1981) was about 4 m tall, the close K_B values for them further meant that even for a relatively tall reactor the form frictional losses in the connecting sections at the bottom and top were significant compared to losses over the heights of riser and downcomer. The external-loop vessel employed by Verlaan *et al.* (1986) had a quite low K_B of 1.81 ± 0.08 even though the A_r/A_d ratio of 4.0 was the same as in one of the devices used by Bello (1981). The explanation lay once again in the geometries of the top and bottom connecting sections used by Verlaan *et al.* (1986): the funnel shaped entrance to downcomer and the smooth radius 90° elbow [as opposed to 90° square elbows used by Bello (1981)] which connected the downcomer to the riser (Verlaan *et al.*, 1986) led to lower pressure losses.

For the internal-loop reactors, Table 1 shows that the order of magnitude of the loss coefficient K_B was quite close for the reactors examined by us, for the draught tube vessels utilized by Bello (1981) and for a similar device studied by Jones (1985). In all these cases the clearance of draught tube (or baffle) from the bottom of the reactor was fairly large at 10–20 cm. The draught tube sparged airlift employed by Hatch (1973) displayed a much higher K_B value at 16.98 ± 3.74, because of the unusually low clearance (only 3.3 cm) of the draught tube from the reactor base. The strong influence of the free area between the riser and the downcomer [i.e. the bottom clearance area (Fig. 2)] on liquid circulation was further evident in Hatch's results where a 67% reduction in this area led to a 32.5% decline in the riser superficial liquid velocity. The coefficient K_B for almost all the several different types of internal-loop airlifts correlated well with the free area for liquid flow between riser and downcomer as shown in Fig. 3. Thus

$$K_B = 11.402\left(\frac{A_d}{A_b}\right)^{0.789} \tag{18}$$

(correlation coefficient = 0.994)

over a A_d/A_b range of 0.2–1.8. Of all the cases examined only one of Bello's (1981) reactors showed K_B values which did not correlate closely with eq. (18). Even for that case, however, the spread of K_B data as shown in Fig. 3 was such that the experimental error in liquid circulation results could easily have been the source of the discrepancy.

The theoretical eq. (16) predicts an increase in liquid circulation with the gas–liquid dispersion height raised to a power of 0.5. Previously Bello *et al.* (1984)

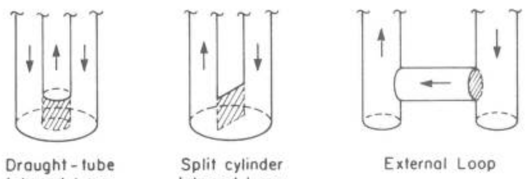

Fig. 2. Free area (hatched) (A_b) available for liquid flow between riser and downcomer in various configurations of bottoms of airlift reactors.

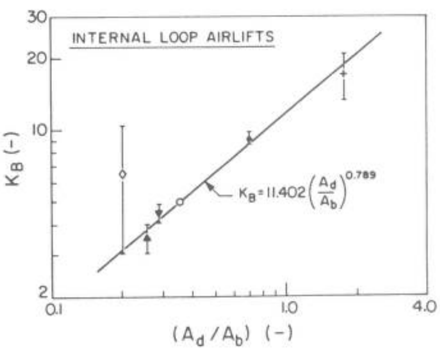

Fig. 3. Correlation of K_B with A_d/A_b for internal-loop airlifts. See Fig. 1 for explanation of symbols.

predicted this exponent to be 1/3 even though all their experiments were conducted in reactors which were operated at a low fixed dispersion height of 1.8 m. No experimental evidence was provided by Bello *et al.* (1984) for their hypothesis. The good agreement of the measured values of liquid circulation, covering a dispersion height range of 1.36 to more than 8 m, with eq. (16) further supports our equation. As a further independent test of eqs (16) and (18), the data obtained in our relatively large split cylinder vessel (reactor 2 in Table 1), which was not used in the development of these equations, was correlated with them. Thus, based on the reactor geometry, eq. (18) was used to calculate K_B which was then used in eq. (16a) to obtain a calculated liquid velocity. The latter was compared with the experimental value. The excellent agreement between these two liquid circulation velocities for this case (Fig. 1) provided additional evidence in support of the theory.

In some cases the riser and downcomer gas holdups may not be known *a priori*. Equation (16) can still be used for liquid velocity prediction although the procedure is now more complex. Because the gas–liquid upflow in the riser of an airlift is identical to concurrent gas–liquid flow in bubble columns, equations developed for the latter can be applied to airlift reactors. Thus, the well-known gas holdup correlation due to Hills (1976) may be rearranged to

$$\varepsilon_r = \frac{U_{Gr}}{0.24 + 1.35(U_{Gr} + U_{Lr})^{0.93}} \tag{19}$$

for $U_{Lr} > 0.3$ m s^{-1} in air–water. Equation (19) is used to calculate ε_r for any given gas velocity using an assumed value for liquid velocity. The downcomer gas holdup is then obtained using

$$\varepsilon_d = 0.89\varepsilon_r \tag{20}$$

or one of the following equations:

$$\varepsilon_d = 0.79\varepsilon_r - 0.057 \tag{21}$$

$$\varepsilon_d = 0.460\varepsilon_r - 0.024. \tag{22}$$

Equations (20) and (21) were reported by Bello *et al.* (1985) for draught tube internal loop and external-loop airlifts, respectively. Equation (22) was obtained in a slightly different form by Chisti *et al.* (1986) also for external loops. Equations (21) and (22) are somewhat dependent on the reactor headspace geometry because of the different gas–liquid separating abilities of different headspace designs. These equations are satisfactory, however, for liquid velocity estimation purposes. The riser and downcomer gas holdups determined using eqs (19)–(22) are now used in eq. (16) for U_{Lr} calculation. If the calculated U_{Lr} and the value that was originally assumed disagree, then the whole procedure is repeated until agreement is obtained.

CONCLUSION

A unified theoretical approach based on energy input into airlift reactors is shown to satisfactorily predict liquid circulation in these devices over a broad range of reactor geometries and scales of operation. For low-viscosity liquids such as water the wall friction has little influence on liquid circulation relative to the frictional losses arising in the top and bottom connecting sections where the flow directions change abruptly. Energy dissipation due to liquid circulation within the wakes behind rising bubbles represents a significant loss. Other major geometric parameters which influence the velocity of liquid circulation are the riser-to-downcomer cross-sectional area ratio, the height of the reactor and A_d/A_b.

Acknowledgement—This work was supported by a research grant from the Natural Sciences and Engineering Research Council of Canada.

NOTATION

A_b	free area for liquid flow between riser and downcomer, m^2
A_d	cross-sectional area (downcomer), m^2
A_r	cross-sectional area (riser), m^2
C_f	Fanning friction factor, dimensionless
DT	draught tube
d_B	bubble diameter, m
d_d	diameter or equivalent diameter (downcomer), m
d_r	diameter or equivalent diameter (riser), m
E_B	energy loss (bottom connection), W
E_D	energy loss due to stagnant gas (downcomer), W
E_F	energy loss due to friction, W
E_i	Energy input, W
E_R	energy loss in wakes (riser), W
E_T	energy loss (top connection), W
g	gravitational acceleration, m s^{-2}
h_D	gas–liquid dispersion height, m
h_L	unaerated liquid height, m
K_B	frictional loss coefficient (bottom), dimensionless
K_T	frictional loss coefficient (top), dimensionless
L_b	downcomer clearance from reactor base, m
L_d	downcomer height, m
L_r	riser height, m
P_h	reactor headspace pressure, N m^{-2}
Q	volumetric gas flow rate, m^3 s^{-1}
U_{Gr}	superficial gas velocity (riser), m s^{-1} [cm s^{-1} in eq. (3)]
U_{Ld}	superficial liquid velocity (downcomer), m s^{-1}
U_{Lr}	superficial liquid velocity (riser), m s^{-1}
V_L	liquid volume, m^3
V_{Ld}	linear (or interstitial) liquid velocity (downcomer), m s^{-1}
V_{Lr}	linear (interstitial) liquid velocity (riser), m s^{-1}

Greek letters

α	coefficient in eqs (2) and (3)
β	coefficient in eq. (2)
ε_d	gas holdup (downcomer), dimensionless
ε_r	gas holdup (riser), dimensionless

Table A1. Energy dissipation in the circulation loop.

U_{Gr} (m s^{-1})	U_{Ld} (m s^{-1})	U_{Lr} (m s^{-1})	ε_r (—)	E_i (W)	$E_R^{\dagger}$ (W)	E_D (W)	$(E_B+E_T)^{\dagger}$ (W)	$E_F^{\dagger}$ (W)
0.010	0.748	0.187	0.017	12.94	9.78 (75.6)	0.0	3.16 (24.5)	0.04 (0.3)
0.022	1.00	0.25	0.0314	28.46	20.65 (72.6)	0.0	7.58 (26.6)	0.09 (0.3)
0.033	1.181	0.295	0.045	42.69	29.49 (69.1)	0.0	12.51 (29.3)	0.15 (0.3)
0.054	1.465	0.366	0.643	69.85	46.45 (66.5)	0.0	23.9 (34.3)	0.27 (0.4)
0.103	1.811	0.453	0.095	133.24	90.44 (67.9)	0.0	45.4 (34.1)	0.52 (0.4)

†Values in parentheses represent percent of E_i.

- η circulation path flow resistance, dimensionless
- μ_{app} apparent viscosity, N m^{-2} s
- μ_L liquid viscosity, N m^{-2} s
- ρ_D dispersion density, kg m^{-3}
- ρ_L liquid density, kg m^{-3}

REFERENCES

Bello, R. A. (1981), Ph.D. thesis, University of Waterloo, Ontario.

Bello, R. A., Robinson, C. W. and Moo-Young, M., 1984, Liquid circulation and mixing characteristics of airlift contactors. *Can. J. chem. Engng* **62**, 573–577.

Bello, R. A., Robinson, C. W. and Moo-Young, M., 1985, Gas holdup and overall volumetric oxygen transfer coefficient in airlift contactors. *Biotechnol. Bioengng* **27**, 369–381.

Blenke, H., 1979, Loop reactors. *Adv. biochem. Engng* **13**, 121–214.

Chakravarty, M., Singh, H. D., Baruah, J. N. and Iyengar, M. S., 1974, Liquid velocity in a gas-lift column. *Indian chem. Engrs* **16**(3), 17–22.

Chisti, M. Y., Fujimoto, K. and Moo-Young, M., 1986, Hydrodynamic and oxygen mass transfer studies in bubble columns and airlift bioreactors. Paper 117a presented at the A.I.Ch.E. Annual Meeting, Miami Beach, 2–7 November.

Fields, P. R., Mitchell, F. R. G. and Slater, N. K. H., 1984, Studies of mixing in a concentric tube air-lift reactor containing xanthan gum by means of an improved flow follower, *Chem. Engng Commun.* **25**, 93–104.

Glasgow, L. A., Erickson, L. E., Lee, C. H. and Patel, S. A., 1984, Wall pressure fluctuations and bubble size distributions at several positions in an airlift fermentor. *Chem. Engng Commun.* **29**, 311–336.

Hatch, R. T., 1973, Ph.D. thesis, Massachusetts Institute of Technology, Cambridge, MA.

Hills, J. H., 1976, The operation of a bubble column at high throughputs I. Gas holdup measurements. *Chem. Engng J.* **12**, 89–99.

Hsu, Y. C. and Dudukovic, M. P., 1980, Gas holdup and liquid circulation in gas-lift reactors. *Chem. Engng Sci.* **35**, 135–141.

Jones, A. G., 1985, Liquid circulation in a draft-tube bubble column. *Chem. Engng Sci.* **40**, 449–462.

Kubota, H., Hosono, Y. and Fujie, K., 1978, Characteristic evaluations of ICI air-lift type deep shaft aerator. *J. chem. Engng Japan* **11**, 319–325.

Lee, C. H., Glasgow, L. A., Erickson, L. E., and Patel, S. A., 1986, Liquid circulation in air-lift fermentors. Paper 8d presented at A.I.Ch.E. Annual Meeting, Miami Beach, 2–7 November.

Levich, V. G., 1962 *Physicochemical Hydrodynamics*, p. 434. Prentice-Hall, Englewood Cliffs, NJ.

Merchuk, J. C. and Stein, Y., 1981, Local hold-up and liquid velocity in air-lift reactors. *A.I.Ch.E. J.* **27**, 377–388.

Onken, U. and Weiland, P., 1980, Hydrodynamics and mass transfer in an airlift loop fermentor. *Eur. J. appl. Microbiol. Biotechnol.* **10**, 31–40.

Popovic, M. and Robinson, C. W., 1984, Estimation of some important design parameters for non-Newtonian liquids in pneumatically agitated fermenters. In *Proceedings of the 34th Canadian Chemical Engineering Congress*, 30th September–3rd October, Quebec City, pp. 258–263.

Verlaan, P., Tramper, J., van't Riet, K. and Luyben, K. Ch. A. M., 1986, Hydrodynamics and axial dispersion in an airlift-loop bioreactor with two and three-phase flow. Paper 07 presented at the International Conference on Bioreactor Fluid Dynamics, Cambridge (England), 15–17 April.

Weiland, P., 1984, Influence of draft tube diameter on operation behaviour of airlift-loop reactors. *Ger. chem. Engng* **7**, 374–385.

APPENDIX 1: ENERGY DISSIPATION IN CIRCULATION LOOP

Shown in Table A1 are some experimental data obtained by Verlaan *et al.* (1986) in air–water in a relatively tall (3.23 m tall) external-loop airlift reactor in which, due to its height, frictional losses are expected to be high. The total energy input E_i was calculated using eq. (5). Verlaan *et al.* (1986) reported the liquid circulation data in terms of the downcomer cross-section and these were converted to the riser superficial liquid velocities using the equation

$$U_{Lr} = U_{Ld}\left(\frac{A_d}{A_r}\right). \tag{A1}$$

The energy loss due to friction over the length of the riser was calculated using

$$E_F = 2C_f \rho_L U_{Lr}(U_{Lr} + U_{Gr})\frac{h_D}{d_r}\cdot(U_{Lr}\cdot A_r) \tag{A2}$$

which was reported by Merchuk and Stein (1981). The Blasius equation

$$C_f = 0.0792\left[\frac{\rho_L U_{Lr} d_r}{(1-\varepsilon_r)\mu_L}\right]^{-0.25} \tag{A3}$$

was employed in the calculation of the Fanning friction factor for use in eq. (A2).

Energy losses due to fluid turn around at the top and bottom of the reactor ($E_T + E_B$) and the losses due to the wakes behind bubbles in the riser (E_R) are also given in Table A1 and these were calculated using eqs (10) and (7), respectively. This particular reactor was operated such that the downcomer gas holdup remained zero and consequently there was no energy dissipation due to bubble drag (E_D) in the downcomer as could be calculated from eq. (9).

As can be seen from Table A1 the energy losses due to wall friction in the riser (E_F) are clearly negligible ($< 1\%$) compared to the energy dissipation due to wakes behind bubbles and that due to the abrupt changes of flow direction in the top and bottom sections of the reactor.